# Supporting Information

# Role of Heteroatom-doping in Enhancing Catalytic Activities and Stability of Single-Atom Catalyst for Oxygen Reduction and Oxygen Evolution Reactions

*Tao Zheng[1]\*, Xiao Han[1], Jincheng Wang[1], Zhenhai Xia[2]\**

[1] State Key Laboratory of Solidification Processing, School of Materials Science and Engineering, Northwestern Polytechnical University, Xi'an, 710072, P.R. China

[2] Department of Materials Science and Engineering, University of North Texas, Denton, TX 76203, USA

\* Corresponding authors: *taozheng@mail.nwpu.edu.cn (T. Zheng);*

*Zhenhai.xia63@gmail.com (Z. Xia)*

## 1. Calculation methods

### 1.1 Reaction pathway

In an acidic environment, the overall 4-electron oxygen reduction reaction (ORR) producing $H_2O$ can be written as:

$$O_2 + 4H^+ + 4e^- \rightarrow 2H_2O \tag{S1}$$

The mechanism of ORR goes through the following elementary steps:

$$O_2 + * \rightarrow O_2^* \tag{S2}$$

$$O_2^* + H^+ + e^- \rightarrow OOH^* \tag{S3}$$

$$OOH^* + H^+ + e^- \rightarrow O^* + H_2O(l) \tag{S4}$$

$$O^* + H^+ + e^- \rightarrow OH^* \tag{S5}$$

$$OH^* + H^+ + e^- \rightarrow H_2O(l) + \ * \tag{S6}$$

As for oxygen evolution reaction (OER), the reaction is the reverse direction of ORR. The overall 4-electron OER in acid environment is:

$$2H_2O \rightarrow O_2 + 4H^+ + 4e^- \tag{S7}$$

The elementary steps are as follow:

$$H_2O(l) + \ * \rightarrow OH^* + H^+ + e^- \tag{S8}$$

$$OH^* \rightarrow O^* + H^+ + e^- \tag{S9}$$

$$O^* + H_2O(l) \rightarrow OOH^* + H^+ + e^- \tag{S10}$$

$$OOH^* \rightarrow O_2^* + H^+ + e^- \tag{S11}$$

$$O_2^* \rightarrow O_2 + \ * \tag{S12}$$

## 1.2 Overpotential

To determine the rate limiting step of ORR on different sites and structures, the free energy change of each step after energy correction can be obtained based on the above elementary steps:

$$\Delta G = \Delta E_{ads}^{DFT} - \Delta ZPE - T\Delta S + \Delta G_U + \Delta G_{pH} \tag{S13}$$

where $\Delta E^{DFT}$ is the DFT-determined energy change of each step, T=293.15 K is the room temperature, and ΔS is the entropy change. ZPE is the zero-point energy of OH*, O* and OOH*, which is calculated with the contribution in the free energy expression considering only vibrational entropy frequencies. In this work, to unify the standard, ZPE were calculated with the fixed substrate to obtain ZPE contribution in the free energy expression.[1] $\Delta G_U = -eU$ is the potential correction, where U is the potential at the electrode. $\Delta G_{pH}$ is the correction of the H$^+$ free energy by the concentration dependence of the entropy:

$$\Delta G_{pH} = -k_B T \ln[\text{H}^+] \tag{S14}$$

where $k_b$ is the Boltzmann constant.

Then, the overpotential $\eta$ of ORR in acid medium (pH=1), is determined by the following equation:

$$\eta_{ORR} = max\{\Delta G_1, \Delta G_2, \Delta G_3, \Delta G_4\}/e + 1.23 \tag{S15}$$

where $\Delta G_1$, $\Delta G_2$, $\Delta G_3$, $\Delta G_4$ are the free energy change of Reaction S3-S6 calculated by Eq. (S13), respectively.

The overpotential $\eta$ of OER in acid medium (pH=1), is calculated by:

$$\eta_{OER} = max\{\Delta G_1, \Delta G_2, \Delta G_3, \Delta G_4\}/e - 1.23 \tag{S16}$$

where $\Delta G_1$, $\Delta G_2$, $\Delta G_3$, $\Delta G_4$ are the free energy change of Reaction S8-S11 calculated by Eq. (S13), respectively.

**1.3 Adsorption energy**

In order to analyze the relationship between the structure and the catalytic activity, the absorption energy of OH*, O* and OOH* were calculated by the following equations:[2]

$$\Delta E_{OH^*} = E(OH^*) - E(*) - \left(E_{H_2O} - 1/2E_{H_2}\right) \tag{S17}$$

$$\Delta E_{O^*} = E(O^*) - E(*) - \left(E_{H_2O} - E_{H_2}\right) \tag{S18}$$

$$\Delta E_{OOH^*} = E(OOH^*) - E(*) - \left(2E_{H_2O} - 3/2E_{H_2}\right) \tag{S19}$$

where $E(*)$ is the ground state energies of a clean surface obtained by DFT calculation, $E(OH^*)$, $E(O^*)$ and $E(OOH^*)$ represent the DFT-calculated energy of surface absorbed with OH*, O* and OOH*, respectively. $E_{H_2O}$ and $E_{H_2}$ are the energies of $H_2O$ and $H_2$ molecules in gas phase obtained by DFT calculation.

## 2. Supplementary Figures
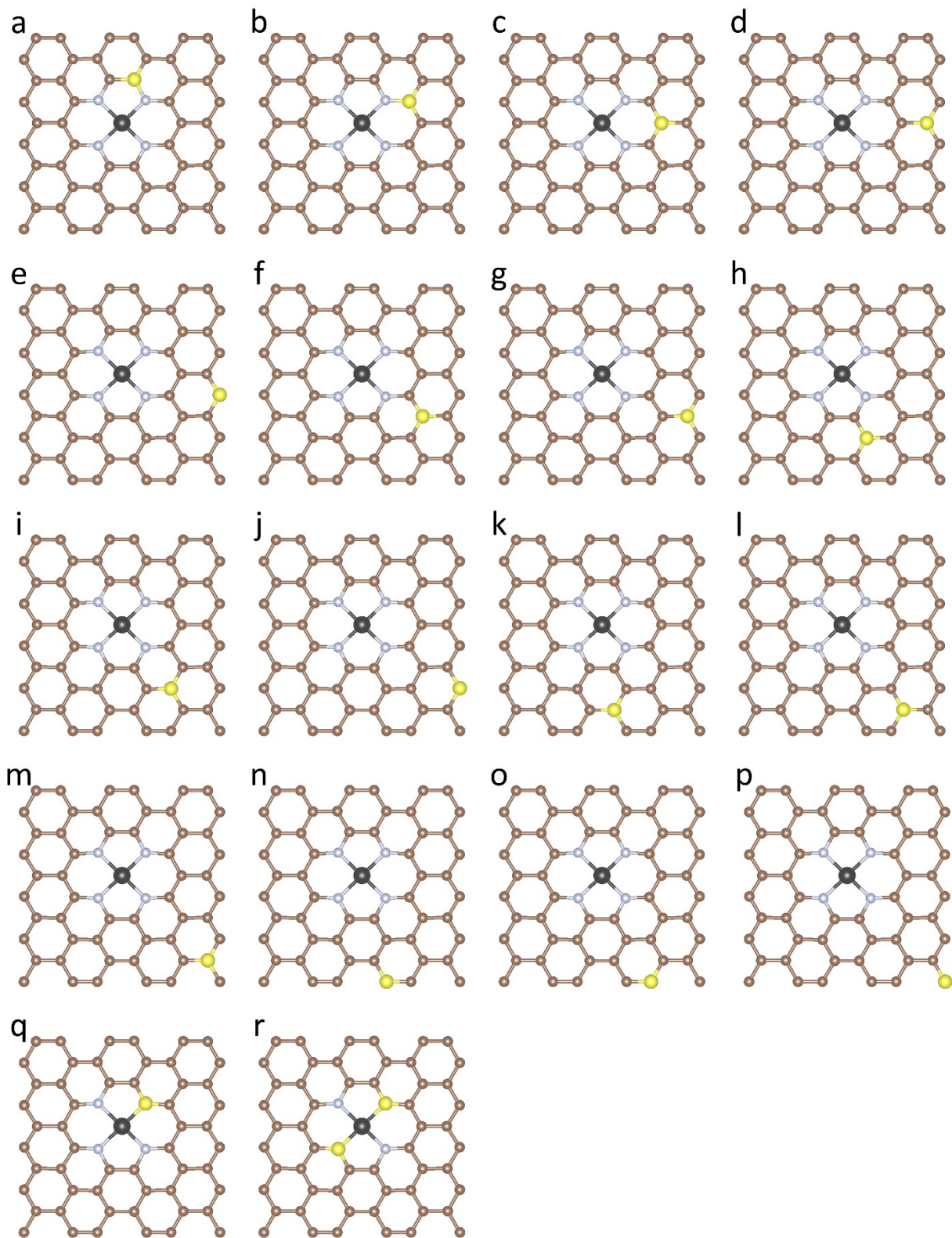
**Fig. S1** The S-doped TM-N-C SAC structure considered in this study. The brown, silver, blue and black balls represent the C, N, S and TM (TM= Sc, Ti, V, Cr, Mn, Fe, Co, Ni, Cu, Zn) atoms, respectively. (a) TM-N-S-1. (b) TM-N-S-2. (c) TM-N-S-3. (d) TM-N-S-4. (e) TM-N-S-5. (f) TM-N-S-6. (g) TM-N-S-7. (h) TM-N-S-8. (i) TM-N-S-9. (j) TM-N-S-10. (k) TM-N-S-11. (l) TM-N-S-12. (m) TM-N-S-13. (n) TM-N-S-14. (o) TM-N-S-15. (p) TM-N-S-16. (q) TM-N$_3$-S. (r) TM-N$_2$-S$_2$.
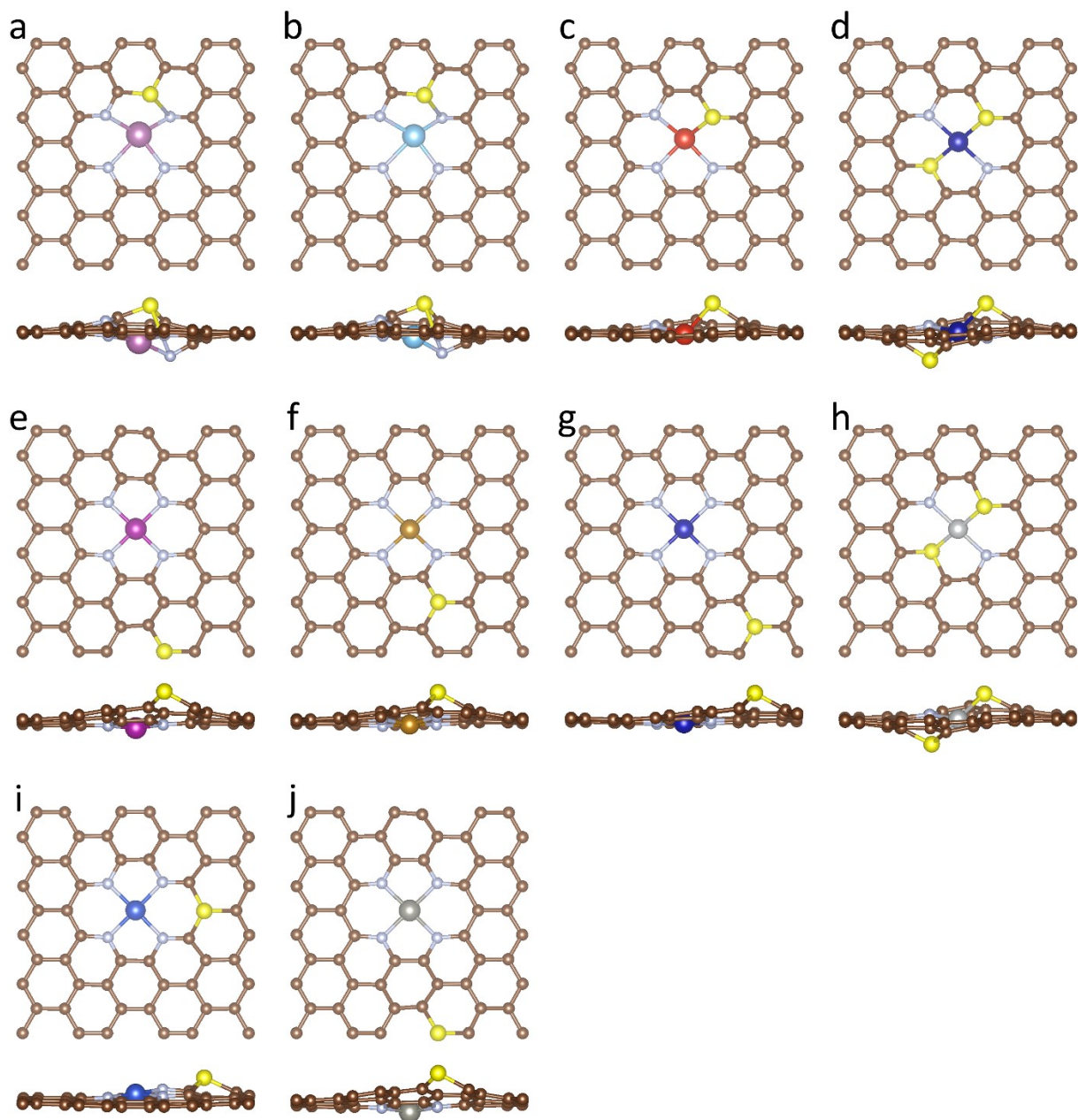
**Fig. S2** The structure with the best ORR overpotential. (a) Sc-N-S-1. (b) Ti-N-S-1. (c) V-N$_3$-S. (d) Cr-N$_2$-S$_2$. (e) Mn-N-S-14. (f) Fe-N-S-8. (g) Co-N-S-12. (h) Ni-N$_2$-S$_2$. (i) Cu-N-S-3. (j) Zn-N-S-14.
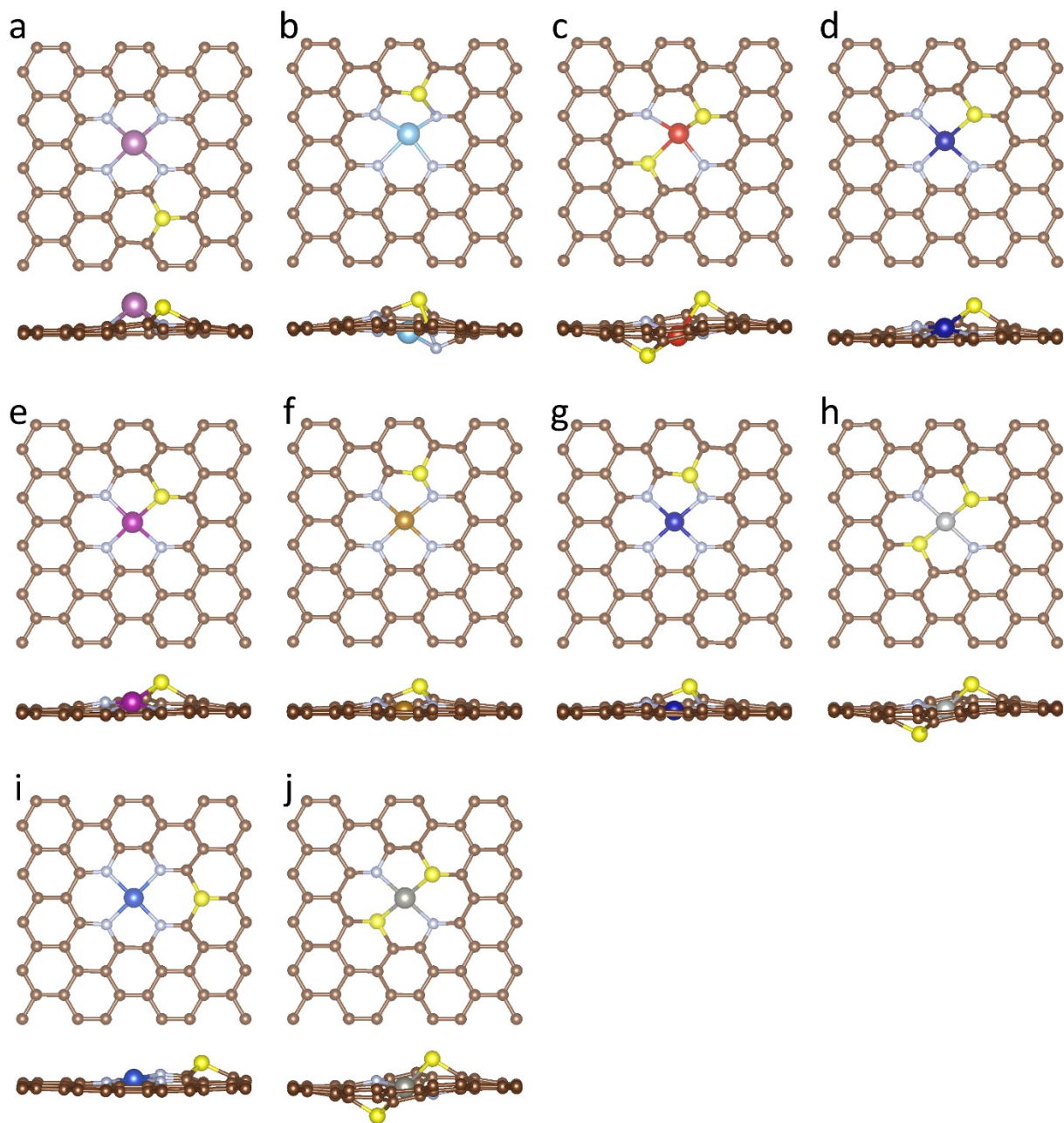
**Fig. S3** The structure with the best OER overpotential. (a) Sc-N-S-8 (b) Ti-N-S-1. (c) V-$N_2$-$S_2$. (d) Cr-$N_3$-S. (e) Mn-$N_3$-S. (f) Fe-N-S-1. (g) Co-N-S-1. (h) Ni-$N_2$-$S_2$. (i) Cu-N-S-3. (j) Zn-$N_2$-$S_2$. It is noted: for Ti, Ni and Cu, the structure with the best ORR and OER overpotential is the same (Ti-N-S-1 in Fig. S3b and S4b, Ni-$N_2$-$S_2$ in Fig. S3h and S4h, Cu-N-S-3 in Fig. S3i and S4i).
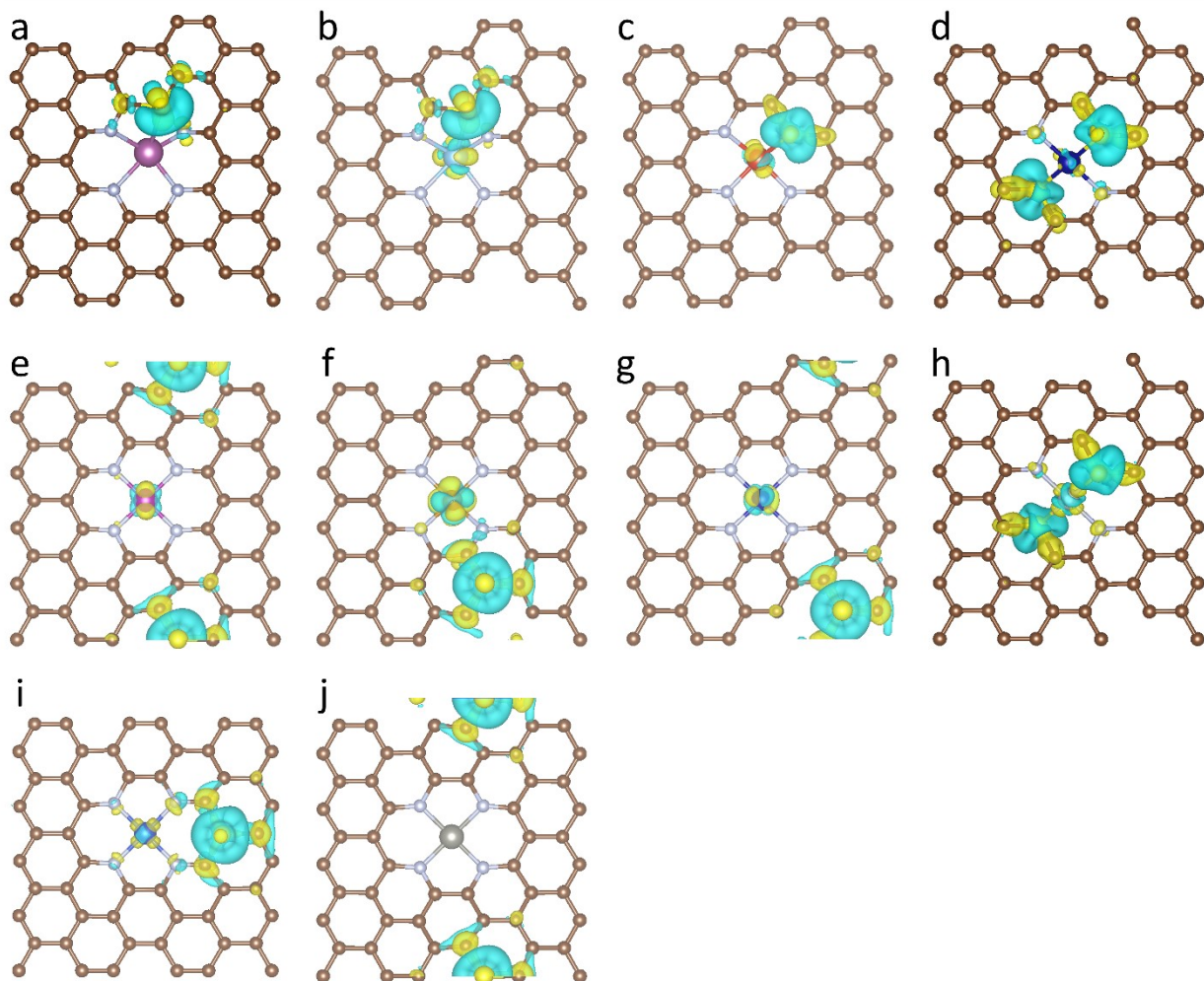
**Fig. S4** The differential charge density distributions (between S-doped and S-undoped structure) of the screened structures corresponding to those shown in Fig. S2 with optimal ORR overpotential.
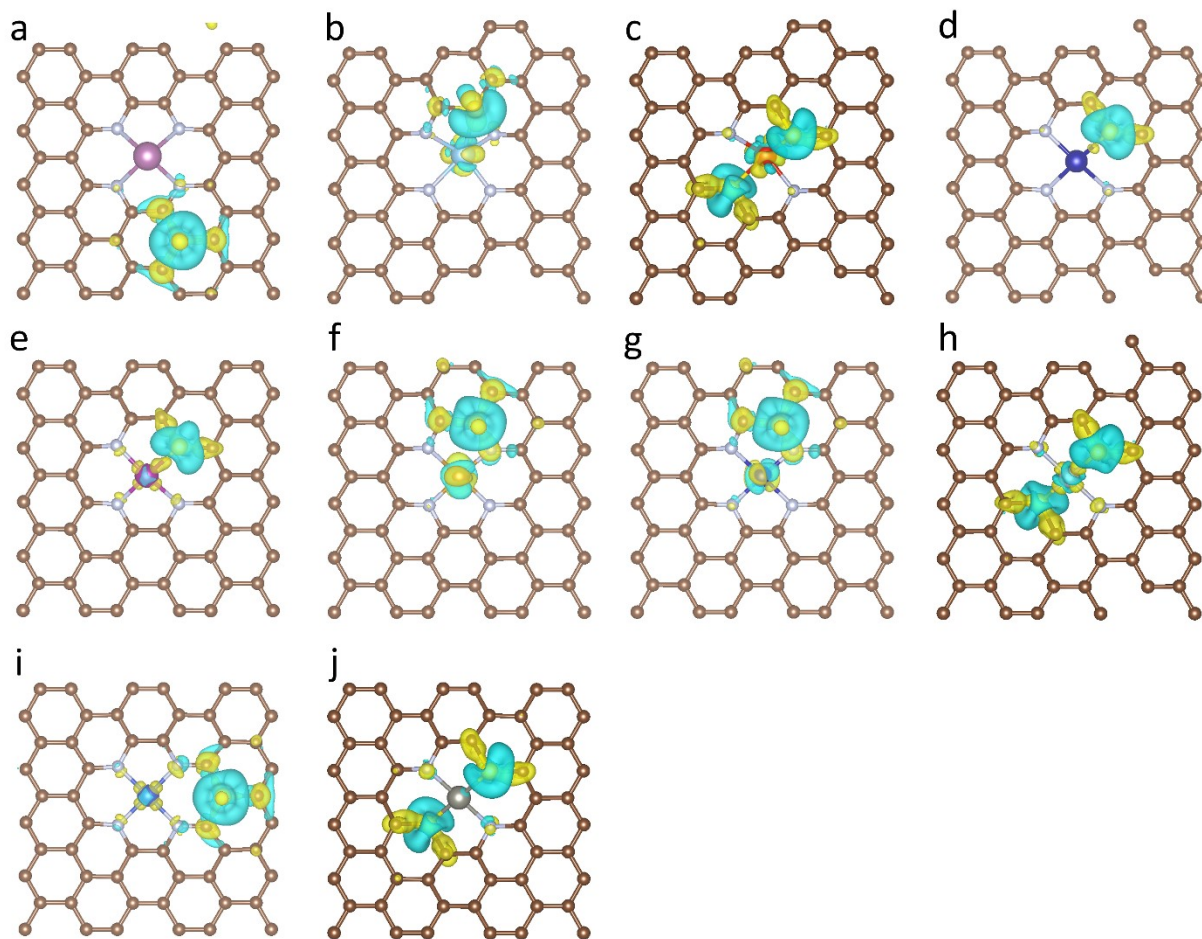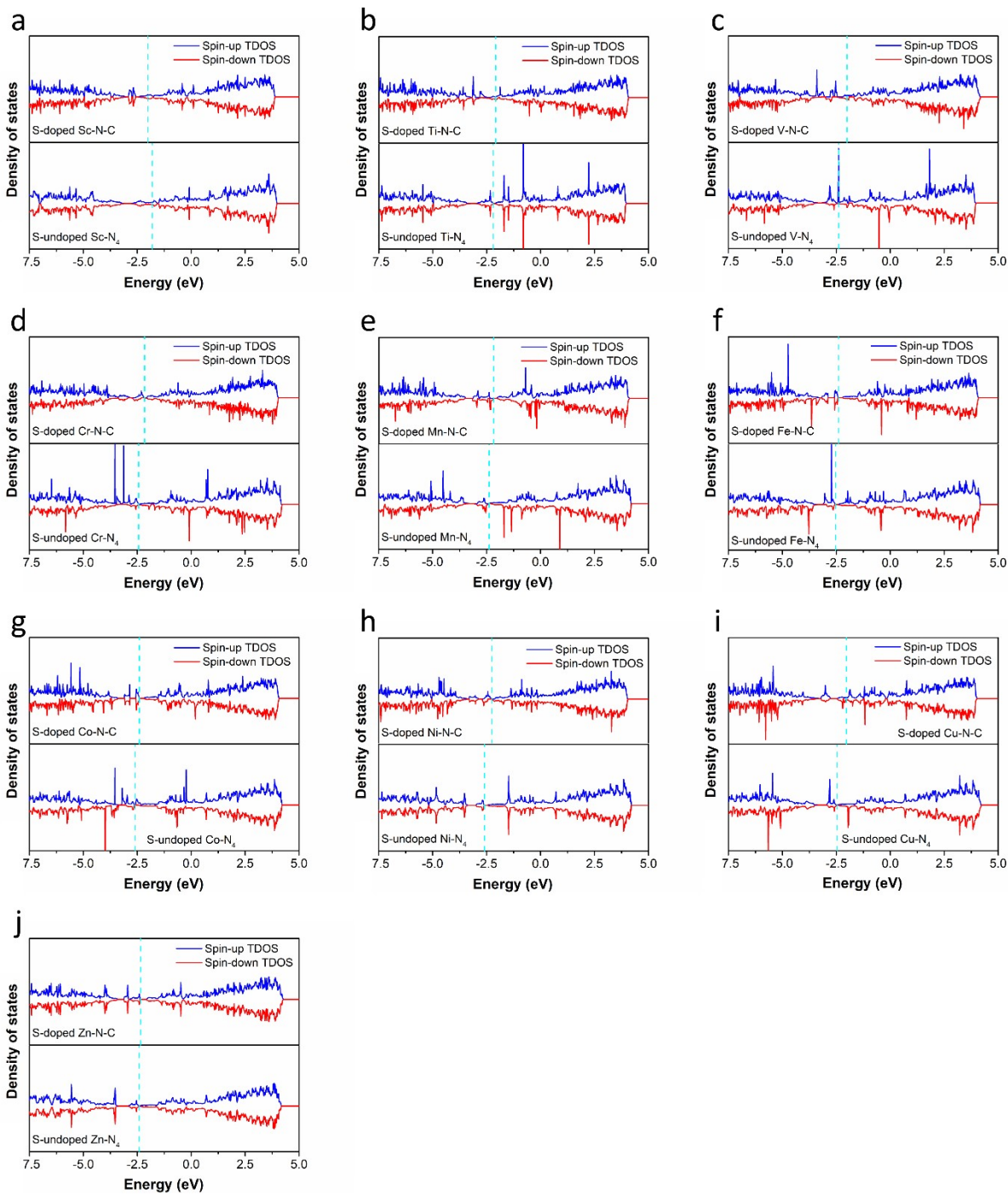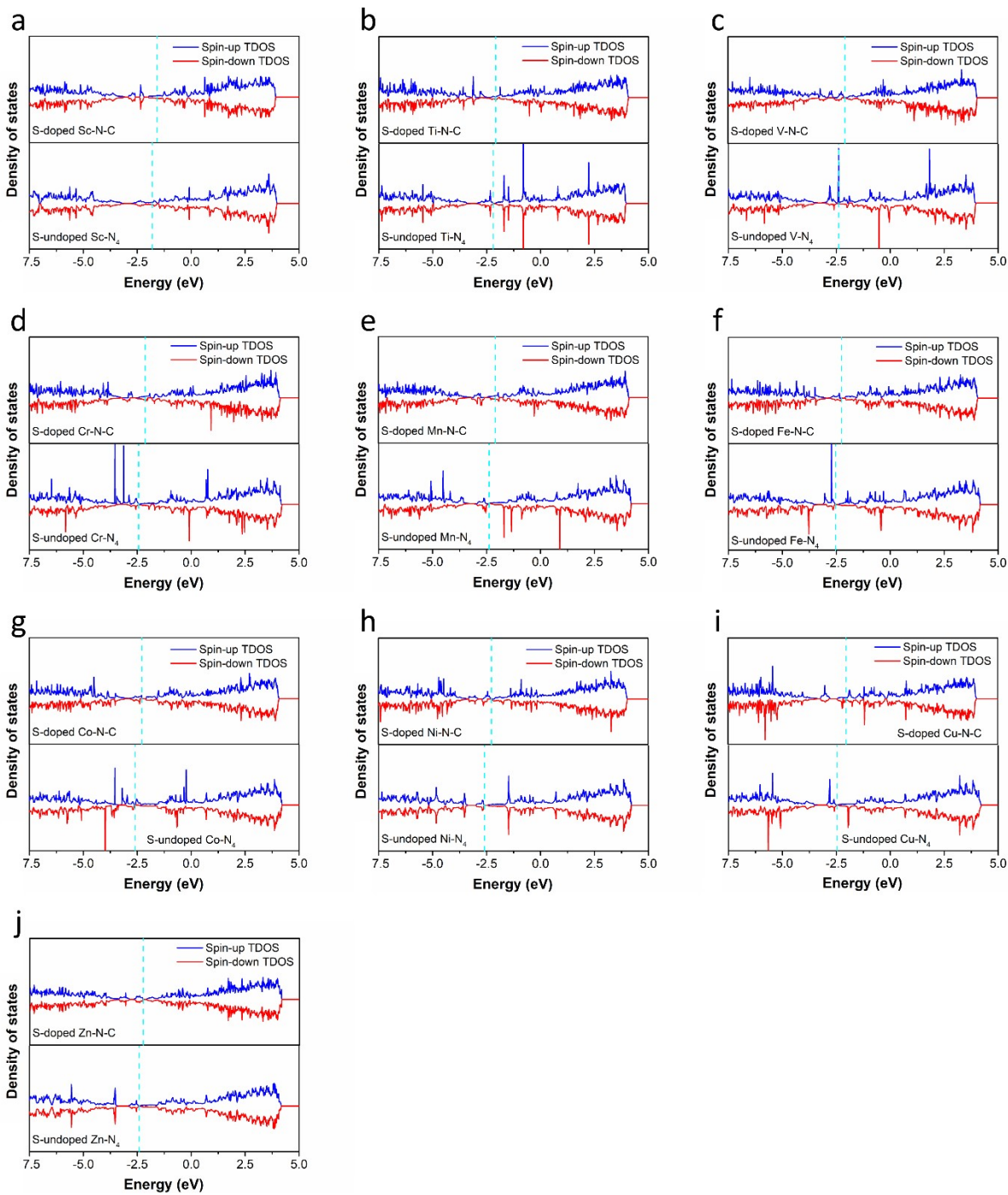
**Fig. S5** The differential charge density distributions (between S-doped and S-undoped structure) of the screened structures (corresponding to those shown in Fig. S3) with optimal OER overpotential.

**Fig. S6** The DOS of the screened structures (corresponding to those shown in Fig. S3) with optimal ORR overpotential. The Fermi energy levels are marked by dotted line.

**Fig. S7** The DOS of the screened structures (corresponding to those shown in Fig. S4) with optimal OER overpotential. The Fermi energy levels are marked by dotted line.

## 3. Supplementary Tables

**Table S1.** The values of U–J used in Hubbard U (DFT+U) corrections:[3]

| TM | Sc | Ti | V | Cr | Mn | Fe | Co | Ni | Cu | Zn |
|----|----|----|----|----|----|----|----|----|----|----|
| U-J | 2.11 | 2.58 | 2.72 | 2.79 | 3.06 | 3.29 | 3.42 | 3.40 | 3.87 | 4.12 |

**Table S2.** The values of valence number ($V_M$, $V_S$, $V_C$), atomic radius ($r_M$, $r_S$, $r_c$) and the descriptors.

| Elements | Valence electron number | Atomic radius (pm) | $\varphi$ | $\varphi^*$ |
|----------|-------------------------|--------------------|-----------|-------------|
| C | 4 | 67 | -- | -- |
| S | 6 | 88 | -- | -- |
| Sc | 3 | 184 | 0.469 | 0.191 |
| Ti | 4 | 176 | -0.12 | 0 |
| V | 5 | 171 | 0 | 0.151 |
| Cr | 6 | 166 | 0.287 | 0.546 |
| Mn | 7 | 161 | 0.674 | 1.107 |
| Fe | 8 | 156 | 1.136 | 1.765 |
| Co | 9 | 152 | 1.671 | 2.515 |
| Ni | 10 | 149 | 2.167 | 3.370 |
| Cu | 11 | 145 | 2.167 | 4.151 |
| Zn | 12 | 142 | 2.707 | 5.012 |

**Reference:**

1. Z. Zhao, M. Li, L. Zhang, L. Dai and Z. Xia, *Adv. Mater.*, 2015, **27**, 6834-6840.
2. M. Li, L. Zhang, Q. Xu, J. Niu and Z. Xia, *J. Catal.*, 2014, **314**, 66-72.

3.      C.-Y. Lin, L. Zhang, Z. Zhao and Z. Xia, *Adv. Mater.*, 2017, **29**, 1606635.